

Can the ERA5 Reanalysis Product Improve the Atmospheric Correction Accuracy of Landsat Series Thermal Infrared Data?

Xiangchen Meng¹, Member, IEEE, Hao Guo, Jie Cheng², Senior Member, IEEE, and Beibei Yao

Abstract—Atmospheric correction is a key step toward estimating land surface temperature from the sensor with only one thermal infrared (TIR) channel. We use ground radiosounding profiles collected from 163 radiosonde observations to provide insights on how well the ERA5 reanalysis product performs in the atmospheric correction of Landsat series TIR data. Despite the poor performance of the ERA5 product for estimating atmospheric upward radiance, downward radiance, and transmittance of Landsat series TIR data in the Americas and Africa, the performance of the ERA5 product was superior to that of the M2I6NPANA (inst6_3d_ana_Np) dataset (MERRA2) and (Final) Operational Global Analysis data (FNL) products in Asia and Europe. The vertical distribution of air temperature and relative humidity profiles may explain the poor performance of ERA5 in the Americas and Africa. This letter shows the advantages and weaknesses of the ERA5 reanalysis product in the atmospheric correction of Landsat series TIR data and will benefit research fields that require an atmospheric profile as input.

Index Terms—Atmospheric correction, European Center for Medium-range Weather Forecasts (ECMWF) reanalysis (ERA5), (Final) Operational Global Analysis data (FNL), M2I6NPANA (inst6_3d_ana_Np) dataset (MERRA2), radiosonde, thermal infrared (TIR).

I. INTRODUCTION

LAND surface temperature (LST) plays an important role in land surface physical processes on regional and global scales [1], [2], which has been widely used in research of hydrology, urban climate, ecology, and so on [3]–[6]. Remote sensing is a unique way of obtaining LST at regional and global scales. As the at-sensor radiance received by a thermal infrared (TIR) channel contains the atmospheric upward and downward radiance [7], it is necessary to correct the atmospheric effects before using the single-channel

Manuscript received January 2, 2022; revised March 9, 2022; accepted April 10, 2022. Date of publication April 14, 2022; date of current version May 3, 2022. This work was supported in part by the Shandong Provincial Natural Science Foundation under Grant ZR2021QD055, in part by the National Natural Science Foundation of China under Grant 42001363 and Grant 42071308, and in part by the Third Xinjiang Scientific Expedition Program under Grant2021XJKK140304. (Corresponding author: Jie Cheng.)

Xiangchen Meng and Hao Guo are with the School of Geography and Tourism, Qufu Normal University, Rizhao, Shandong 276826, China, and also with the Rizhao Key Laboratory of Territory Spatial Planning and Ecological Construction, Qufu Normal University, Rizhao 276825, China (e-mail: xiangchenmeng@qfnu.edu.cn; guohao@qfnu.edu.cn).

Jie Cheng is with the State Key Laboratory of Remote Sensing Science, Faculty of Geographical Science, Beijing Normal University, Beijing 100875, China, and also with the Faculty of Geographical Science, Institute of Remote Sensing Science and Engineering, Beijing Normal University, Beijing 100875, China (e-mail: Jie_Cheng@bnu.edu.cn).

Beibei Yao is with the School of Marxism, Qufu Normal University, Rizhao, Shandong 276826, China (e-mail: beibeiyao@qfnu.edu.cn).

Digital Object Identifier 10.1109/LGRS.2022.3167388

algorithm and the multichannel algorithm for LST inversion. Global reanalysis products were widely used to implement the atmospheric correction, considering its long observation period and good data quality. For example, Barsi *et al.* [8] and Tardy *et al.* [9] developed an atmospheric correction tool for Landsat TIR data using the National Centers for Environmental Prediction (NCEP) and the European Center for Medium-range Weather Forecasts (ECMWF) Interim Reanalysis (ERA-Interim) product, respectively. Cheng *et al.* [10] and Malakar *et al.* [11] used the National Aeronautics and Space Administration (NASA) Modern Era Reanalysis for Research and Applications Version-2 (MERRA-2) reanalysis data to perform atmospheric correction before producing LST products. Hulley *et al.* [12] and Zhou and Cheng [13] used MERRA-2 reanalysis data to correct the atmospheric effects before acquiring LST from the Visible Infrared Imager Radiometer Suite (VIIRS) and Advanced Himawari Imager (AHI) data, respectively, using the temperature and emissivity separation algorithm. In addition, researchers also evaluated the accuracy of atmospheric profiles from different reanalysis and satellite-derived products [14]–[18].

In our previous research, ERA-Interim and MERRA reanalysis products were accurate than other reanalysis products in the atmospheric correction of Landsat 8 TIR data [15]. As the official replacement of ERA-Interim, the newly released fifth- (and latest) generation ECMWF reanalysis (ERA5) provides alternative input data for atmospheric correction of TIR data. Although ERA5 provides a global improvement with several different technical changes and innovations [19], the exploration of the ERA5 reanalysis product is still insufficient, especially in the atmospheric correction of TIR data.

Assessing the accuracy of the ERA5 reanalysis product will help encourage its use in LST inversion. This study aims to evaluate the utility of the ERA5 reanalysis product in the atmospheric correction of Landsat series TIR data. This letter is organized as follows: Section II introduces the used global radiosonde observations, reanalysis products, and atmospheric parameter simulation with MODTRAN. Section III provides the validation results and analysis. Sections IV and V show the discussion and conclusions of this study.

II. DATA AND PREPROCESSING

A. Global Radiosonde Observations

The radiosounding profiles were collected from 163 global radiosonde stations and downloaded from <http://weather.uwyo.edu/upperair/sounding.html>. In this study, a total of 34 438 valid radiosounding profiles were obtained. In addition to the profiles used in our previous

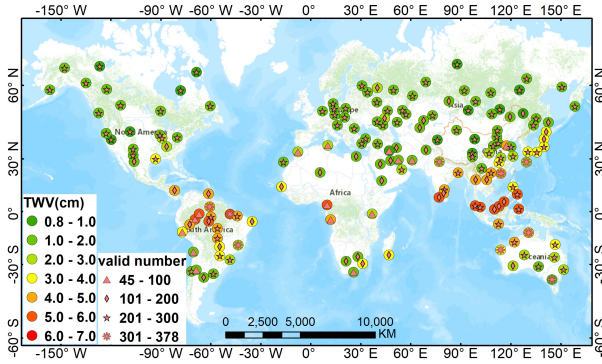


Fig. 1. Spatial distribution of 163 radiosonde stations. The colored circular symbols and medium coral polygonal symbols, respectively, represent the average TWV content and the valid number of radiosounding profiles at each station.

research [10], [15], radiosounding profiles with high total water vapor (TWV) content were incorporated to improve the representativeness of the samples, including 544 profiles in 2013 and 3036 profiles in 2018. Fig. 1 shows the spatial distribution of 163 global radiosonde stations, the corresponding average TWVs, and the valid number of radiosounding profiles at each station. As shown in Fig. 1, there are 94 radiosonde stations with an average TWV less than 2 cm, 36 radiosonde stations with an average TWV between 2 and 4 cm, and 33 radiosonde stations with an average TWV greater than 4 cm. The valid number of radiosounding profiles at most sites is greater than 200, and 15 sites with a valid number of less than 100 are located in Africa and South America.

B. Global Reanalysis Products

ERA5 is the fifth-generation ECMWF atmospheric reanalysis of the global climate covering the past four to seven decades. The dataset used in this study is ERA5 hourly data on pressure levels from 1979 to the present (hereafter ERA5), which provides global, hourly estimates of atmospheric variables, at a horizontal resolution of 0.25° and 37 pressure levels from 1000 to 1 hPa [20].

MERRA version 2 is a NASA atmospheric reanalysis that covers the period from 1980 onward. In this letter, the M2I6NPANA (inst6_3d_ana_Np) [21] dataset (MERRA2) is used. MERRA2 is the analyzed meteorological fields for 42 pressure levels at the native resolution of 0.625° longitude \times 0.5° latitude [15]. Each reanalysis file contains the following times compacted into a daily file: 00, 06, 12, and 18 Coordinated Universal Time (UTC).

The archived NCEP Final Global Data Assimilation System Operational Global Analysis data [hereafter (Final) Operational Global Analysis data (FNL)] provides estimated atmospheric variables every 6 h, with a horizontal resolution of 1.0° and 21 pressure levels from 1000 to 100 hPa [22].

The ERA5, MERRA2, and FNL datasets can be downloaded from the following websites: <https://cds.climate.copernicus.eu/>, <https://disk.sci.gsfc.nasa.gov/>, and <https://rda.ucar.edu/>.

C. Atmospheric Parameter Simulation With MODTRAN

We followed the method proposed by Barsi *et al.* [8] and Li *et al.* [16] to extract the profiles from the global reanalysis

TABLE I
EVALUATION RESULT OF ATMOSPHERIC UPWARD RADIANCE (L^\uparrow), DOWNWARD RADIANCE (L^\downarrow), AND TRANSMITTANCE (τ) FOR LANDSAT 5/7/8 TIR DATA. THE UNIT OF L^\uparrow IS $W/(m^2 \cdot \mu m \cdot sr)$, AND τ IS UNITLESS

		Landsat5/7/8		
		ERA5	MERRA2	FNL
L^\uparrow	Bias	-0.18/-0.18/-0.18	-0.08/-0.08/-0.08	-0.11/-0.11/-0.11
	RMSE	0.69/0.67/0.65	0.31/0.31/0.31	0.32/0.32/0.32
L^\downarrow	Bias	-0.23/-0.24/-0.24	-0.10/-0.10/-0.10	-0.14/-0.14/-0.14
	RMSE	0.92/0.91/0.90	0.40/0.39/0.40	0.41/0.41/0.41
τ	Bias	0.02/0.02/0.02	0.01/0.01/0.01	0.01/0.01/0.01
	RMSE	0.09/0.09/0.08	0.04/0.04/0.04	0.04/0.04/0.04

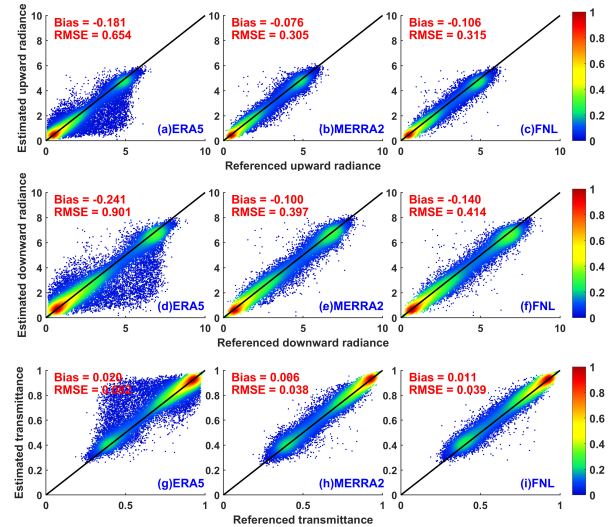


Fig. 2. Evaluation results of (a)–(c) atmospheric upward radiance, (d)–(f) downward radiance, and (g)–(i) transmittance for Landsat 8 simulated from the ERA5, MERRA-2, and FNL reanalysis products. The units of the atmospheric upward (downward) radiance and transmittance are $W/(m^2 \cdot \mu m \cdot sr)$ and unitless, respectively. Statistical metrics are given in each panel: the mean difference (Bias) and the RMSE. The solid lines are the 1:1 lines.

data. First, the atmosphere profiles were extracted according to the observation time (00/12 UTC) of radiosonde stations. Second, the atmosphere profiles surrounding the radiosonde stations were extracted using the nearest-neighbor interpolation method. Finally, the extracted atmospheric profiles were then input into MODTRAN to compute three atmospheric parameters (atmospheric upward radiance, downward radiance, and transmittance) for TIR channels of Landsat series. Detailed information about the above process, refer to our previous research [15]. The performance of the global reanalysis products was assessed through two error metrics: the mean difference (Bias) and the root mean square error (RMSE), which were calculated by taking the atmospheric parameters simulated from radiosounding profiles as a reference.

III. RESULTS AND ANALYSIS

A. Overall Evaluation Results of the Simulated Atmospheric Parameters

The evaluation results of the simulated atmospheric upward radiance, downward radiance, and transmittance for Landsat 5/7/8 TIR channel using three reanalysis products are shown in Table I and Fig. 2, respectively.

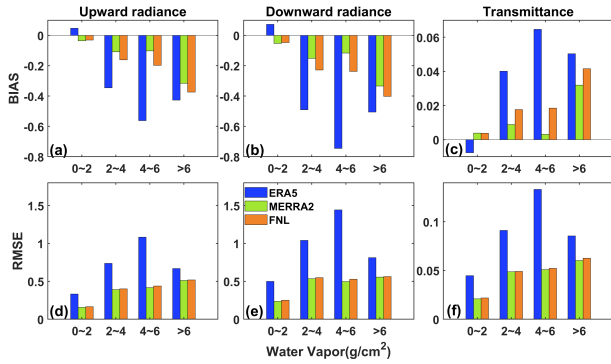


Fig. 3. Histograms of (a)–(c) biases and (d)–(f) RMSEs between the atmospheric upward radiance, downward radiance, and transmittance of Landsat 8 simulated from the ERA5 (blue), MERRA2 (green), FNL (orange) reanalysis product and that simulated from radiosonde observations. The units of the atmospheric upward (downward) radiance and transmittance are $W/(m^2 \cdot \mu m \cdot sr)$ and unitless, respectively.

As shown in Fig. 2, there are obvious outliers in three atmospheric parameters simulated from the ERA5 reanalysis product, while the results simulated using MERRA2 and FNL reanalysis products have fewer outliers. Compared with the atmospheric parameters simulated from radiosounding profiles, the atmospheric upward radiance and downward radiance simulated from three reanalysis products were underestimated, and the atmospheric transmittance was just the opposite. The overall biases were between -0.08 (-0.10) and -0.18 (-0.24) $W/(m^2 \cdot \mu m \cdot sr)$, 0.01 and 0.02 for the atmospheric upward (downward) radiance and transmittance of Landsat 8, respectively, whereas the overall RMSEs were between 0.31 (0.40) and 0.65 (0.90) $W/(m^2 \cdot \mu m \cdot sr)$, 0.04 and 0.08 for Landsat 8, respectively. As shown in Table I, the overall biases (RMSEs) of three atmospheric parameters for Landsat 5/7 are similar to that of Landsat 8.

The overall evaluation results indicated that despite the higher temporal and spatial resolution of ERA5, the uncertainty of three atmospheric parameters simulated from ERA5 reanalysis product was higher than that simulated using the MERRA2 and FNL reanalysis products. The accuracy of three atmospheric parameters simulated from MERRA2 was slightly higher than that simulated from FNL, which was consistent with our previous conclusion [15].

B. Atmospheric Parameters' Evaluation Results Under Various Water Vapor Contents

Just like our previous researches [10], [15], the accuracy of three atmospheric parameters was evaluated in four groups of TWV: $TWV \leq 2$ g/cm^2 , $2 < TWV \leq 4$ g/cm^2 , $4 < TWV \leq 6$ g/cm^2 , and $TWV > 6$ g/cm^2 . The evaluation results of atmospheric parameters for various water vapor contents are shown in Fig. 3 and Table II.

As indicated in Fig. 3, when the TWV was between 0 and 2 g/cm^2 , the atmospheric upward radiance and downward radiance of Landsat 8 simulated from ERA5 reanalysis product were overestimated by approximately 0.05 and 0.07 $W/(m^2 \cdot \mu m \cdot sr)$, whereas the atmospheric upward (downward) radiance simulated from the MERRA2 and FNL reanalysis products was underestimated by approximately 0.04 (0.05) and 0.03 (0.05) $W/(m^2 \cdot \mu m \cdot sr)$. When TWV was

TABLE II

BIASES (RMSEs) BETWEEN THE ATMOSPHERIC UPWARD RADIANCE (L^\uparrow), DOWNWARD RADIANCE (L^\downarrow), AND TRANSMITTANCE (τ) OF LANDSAT 5/7 SIMULATED FROM ERA5, MERRA2, AND FNL REANALYSIS PRODUCTS AND THAT SIMULATED FROM RADIOSONDE OBSERVATIONS. THE UNIT OF L^\uparrow (L^\downarrow) IS $W/(m^2 \cdot \mu m \cdot sr)$, AND τ IS UNITLESS

twv	Bias of Landsat 5/7			RMSE of Landsat 5/7			
	ERA5	MERRA2	FNL	ERA5	MERRA2	FNL	
L^\uparrow	0-2	0.05/0.05	-0.04/-0.04	-0.03/-0.03	0.38/0.37	0.18/0.17	0.19/0.18
	2~4	-0.38/-0.37	-0.12/-0.12	-0.17/-0.17	0.80/0.77	0.41/0.40	0.42/0.41
	4~6	-0.56/-0.56	-0.11/-0.11	-0.19/-0.19	1.09/1.08	0.40/0.40	0.42/0.42
	>6	-0.39/-0.40	-0.29/-0.30	-0.34/-0.35	0.63/0.63	0.47/0.48	0.48/0.48
L^\downarrow	0-2	0.09/0.08	-0.06/-0.06	-0.05/-0.05	0.56/0.54	0.27/0.26	0.28/0.27
	2~4	-0.52/-0.51	-0.16/-0.16	-0.24/-0.23	1.09/1.06	0.54/0.53	0.56/0.55
	4~6	-0.72/-0.72	-0.11/-0.11	-0.22/-0.22	1.42/1.41	0.45/0.46	0.48/0.49
	>6	-0.45/-0.46	-0.29/-0.30	-0.34/-0.36	0.74/0.75	0.49/0.50	0.49/0.51
τ	0-2	-0.01/-0.01	5e-3/5e-3	4e-3/4e-3	0.05/0.05	0.02/0.02	0.03/0.02
	2~4	0.04/0.04	0.01/0.01	0.02/0.02	0.10/0.10	0.05/0.05	0.05/0.05
	4~6	0.07/0.07	3e-3/3e-3	0.02/0.02	0.14/0.14	0.05/0.05	0.05/0.05
	>6	0.05/0.05	0.03/0.03	0.04/0.04	0.08/0.08	0.06/0.06	0.06/0.06

larger than 2 g/cm^2 , the atmospheric upward radiance and downward radiance of Landsat 8 simulated from three reanalysis products were underestimated, and the atmospheric transmittance was just the opposite.

As shown in Table II, the accuracy of three atmospheric parameters simulated from MERRA2 in each subrange of TWV was slightly higher than that simulated from FNL and much higher than that simulated from ERA5. The biases (RMSEs) of three atmospheric parameters at four groups of TWV for Landsat 5/7 were comparable to that of Landsat 8. Like the evaluation results of three atmospheric parameters for Landsat 8, when $TWV \leq 2$ g/cm^2 , the atmospheric upward (downward) radiance and transmittance for Landsat 5/7 simulated from MERRA2 (FNL) were underestimated and overestimated, respectively, whereas those values were just the opposite for that simulated from ERA5. When $TWV > 2$ g/cm^2 , three atmospheric parameters for Landsat 5/7 simulated from MERRA2, FNL, and ERA5 were just the opposite to those when $TWV \leq 2$ g/cm^2 . Compared with the evaluation results of MERRA2 and FNL, ERA5 had maximum RMSE values for three atmospheric parameters, which were about 1.3, 2.0, and 2.6 times higher than those simulated from MERRA2 and FNL when $TWV > 6$ g/cm^2 , $TWV \leq 4$ g/cm^2 , and $4 < TWV \leq 6$ g/cm^2 , respectively.

Based on the aforementioned analysis, the absolute biases (RMSEs) of three atmospheric parameters for Landsat 5/7/8 simulated from MERRA2 and FNL were lower than those simulated from ERA5 in each subrange of TWV. In general, the accuracy of three atmospheric parameters for Landsat 5/7/8 simulated from MERRA2, FNL, and ERA5 gradually decreased.

C. Atmospheric Parameters' Evaluation Results in Six Continents

Reanalysis products may perform differently over regions; the biases and RMSEs of atmospheric parameters simulated from the ERA5, MERRA2, and FNL reanalysis products in six continents were calculated and are shown in Tables III and IV, respectively.

Based on Table III, three atmospheric parameters simulated from the ERA5 product had the lowest absolute biases in

TABLE III

AVERAGE BIASES OF THE ATMOSPHERIC UPWARD RADIANCE (L^\uparrow), DOWNWARD RADIANCE (L^\downarrow), AND TRANSMITTANCE (τ) FOR LANDSAT 5/7/8 IN SIX CONTINENTS. THE UNIT OF L^\uparrow (L^\downarrow) IS $W/(m^2 \cdot \mu m \cdot sr)$, AND τ IS UNITLESS

	Landsat 5/7/8			
	ERA5	MERRA2	FNL	
L^\uparrow	NA	-0.04/-0.04/-0.06	-0.06/-0.05/-0.05	-0.07/-0.07/-0.07
	SA	-0.88/-0.86/-0.86	-0.08/-0.08/-0.07	-0.17/-0.17/-0.17
	AF	-0.21/-0.20/-0.19	-0.11/-0.10/-0.10	-0.15/-0.15/-0.14
	EU	-0.05/-0.05/-0.05	-0.04/-0.04/-0.04	-0.05/-0.05/-0.04
	AS	-0.08/-0.08/-0.08	-0.11/-0.10/-0.10	-0.12/-0.12/-0.12
	OA	-0.15/-0.14/-0.14	-0.06/-0.06/-0.05	-0.12/-0.11/-0.11
L^\downarrow	NA	-0.02/-0.03/-0.05	-0.08/-0.08/-0.07	-0.09/-0.09/-0.09
	SA	-1.18/-1.17/-1.18	-0.10/-0.10/-0.10	-0.20/-0.20/-0.21
	AF	-0.26/-0.25/-0.25	-0.14/-0.14/-0.13	-0.20/-0.20/-0.20
	EU	-0.07/-0.07/-0.07	-0.06/-0.06/-0.05	-0.06/-0.06/-0.06
	AS	-0.10/-0.10/-0.10	-0.13/-0.13/-0.13	-0.15/-0.15/-0.15
	OA	-0.18/-0.18/-0.18	-0.07/-0.07/-0.07	-0.14/-0.14/-0.14
τ	NA	0.00/0.00/0.01	0.01/0.01/0.01	0.01/0.01/0.01
	SA	0.11/0.10/0.10	0.00/0.00/0.00	0.02/0.02/0.02
	AF	0.02/0.02/0.02	0.01/0.01/0.01	0.02/0.02/0.02
	EU	0.01/0.01/0.01	0.00/0.00/0.00	0.01/0.01/0.01
	AS	0.01/0.01/0.01	0.01/0.01/0.01	0.01/0.01/0.01
	OA	0.01/0.01/0.01	0.00/0.00/0.00	0.01/0.01/0.01

North America(NA), South America(SA), Africa(AF), Europe(EU), Asia(AS), Oceania(OA)

TABLE IV

AVERAGE RMSES OF THE ATMOSPHERIC UPWARD RADIANCE (L^\uparrow), DOWNWARD RADIANCE (L^\downarrow), AND TRANSMITTANCE (τ) FOR LANDSAT 5/7/8 IN SIX CONTINENTS. THE UNIT OF L^\uparrow (L^\downarrow) IS $W/(m^2 \cdot \mu m \cdot sr)$, AND τ IS UNITLESS

	Landsat 5/7/8			
	ERA5	MERRA2	FNL	
L^\uparrow	NA	0.96/0.92/0.87	0.21/0.20/0.19	0.23/0.22/0.22
	SA	1.44/1.41/1.39	0.38/0.38/0.38	0.41/0.40/0.41
	AF	0.66/0.64/0.62	0.36/0.35/0.34	0.37/0.36/0.35
	EU	0.18/0.17/0.16	0.21/0.20/0.19	0.21/0.20/0.19
	AS	0.28/0.28/0.28	0.34/0.34/0.34	0.35/0.35/0.35
	OA	0.26/0.26/0.25	0.30/0.30/0.30	0.30/0.30/0.29
L^\downarrow	NA	1.32/1.29/1.24	0.28/0.28/0.27	0.31/0.31/0.30
	SA	1.93/1.90/1.91	0.47/0.47/0.49	0.50/0.51/0.52
	AF	0.90/0.88/0.87	0.48/0.47/0.46	0.50/0.49/0.48
	EU	0.25/0.24/0.23	0.29/0.28/0.27	0.30/0.29/0.28
	AS	0.34/0.34/0.35	0.43/0.43/0.43	0.44/0.44/0.45
	OA	0.32/0.32/0.32	0.37/0.37/0.38	0.37/0.37/0.37
τ	NA	0.13/0.12/0.11	0.03/0.03/0.02	0.03/0.03/0.03
	SA	0.18/0.18/0.17	0.05/0.05/0.05	0.05/0.05/0.05
	AF	0.08/0.08/0.08	0.05/0.04/0.04	0.05/0.05/0.04
	EU	0.02/0.02/0.02	0.03/0.03/0.03	0.03/0.03/0.03
	AS	0.03/0.03/0.03	0.04/0.04/0.04	0.04/0.04/0.04
	OA	0.03/0.03/0.03	0.04/0.04/0.04	0.04/0.04/0.04

North America(NA), South America(SA), Africa(AF), Europe(EU), Asia(AS), Oceania(OA)

Asia, followed by those simulated from the MERRA2 and FNL products. The absolute biases of three atmospheric parameters for the ERA5 product in South America, Africa, and Oceania were higher than those for the MERRA2 and FNL products. The absolute biases of three atmospheric parameters for three reanalysis products were comparable in Europe and North America. Based on Table IV, the performance of the ERA5 product in six continents showed two extremes: 1) the ERA5 product had the lowest RMSE in Asia, Europe, and Oceania, followed by the MERRA2 and FNL products and 2) as for North America, South America, and Africa, the ERA5 and MERRA products had the highest and lowest RMSEs, respectively.

The aforementioned results indicated that compared with the MERRA and FNL products, the ERA5 product can obtain better or similar atmospheric correction accuracy of Land-

TABLE V

BIASES OF THE ATMOSPHERIC UPWARD RADIANCE (L^\uparrow), DOWNWARD RADIANCE (L^\downarrow), AND TRANSMITTANCE (τ) FOR LANDSAT 5/7/8 FOR THREE STATIONS. THE UNIT OF L^\uparrow (L^\downarrow) IS $W/(m^2 \cdot \mu m \cdot sr)$, AND τ IS UNITLESS

	ID	Landsat 5/7/8		
		ERA5	MERRA2	FNL
L^\uparrow	61641	0.43/0.42/0.40	-0.23/-0.23/-0.21	-0.40/-0.38/-0.36
	72240	-2.70/-2.62/-2.58	-0.46/-0.46/-0.46	-0.44/-0.43/-0.44
	84628	-0.45/-0.44/-0.41	-1.02/-0.98/-0.91	0.11/0.11/0.11
L^\downarrow	61641	0.79/0.76/0.70	-0.29/-0.29/-0.28	-0.53/-0.52/-0.50
	72240	-3.51/-3.44/-3.50	-0.56/-0.56/-0.59	-0.54/-0.55/-0.57
	84628	-0.59/-0.58/-0.56	-1.32/-1.28/-1.24	0.20/0.19/0.18
τ	61641	-0.05/-0.05/-0.04	0.02/0.02/0.02	0.04/0.04/0.04
	72240	0.33/0.32/0.31	0.05/0.05/0.05	0.04/0.04/0.04
	84628	0.07/0.07/0.06	0.13/0.12/0.11	0.00/0.00/0.00

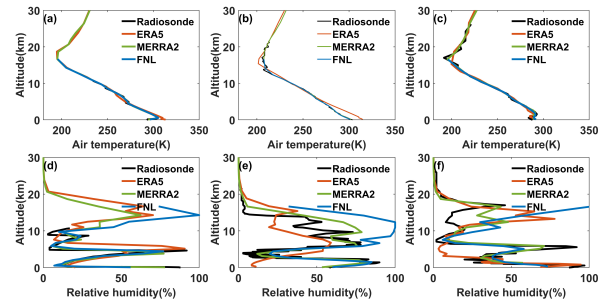


Fig. 4. Vertical distribution of (a)–(c) air temperature and (d)–(f) relative humidity extracted from different atmospheric profiles on (a) and (f) 15 April 2013 at Dakar station, (b) and (e) 15 July 2013 at Lake Charles station, and (c) and (f) 15 July 2013 at Lima–Callao station.

sat series TIR data in most regions except in the Americas and Africa.

IV. DISCUSSION

A. Necessity of Atmospheric Correction for the TIR Channel

Accurate satellite retrieval of LST is difficult to achieve without proper correction of atmospheric effects. The TIR atmospheric corrections consist of correcting the radiance measured by the sensors for the effects of atmospheric attenuation, emission, and emission–reflection [7], which can cause apparent surface temperatures to deviate from actual temperatures by 10 K or more [23]. In addition, in the visible–near-infrared band, the scattering of aerosol is a critical component in atmospheric correction, but for the TIR band under clear-sky conditions, the atmospheric effects caused by water vapor absorption and thermal radiation of the atmosphere itself should be corrected. Therefore, although atmospheric scattering in the TIR channel is low, atmospheric effects must be corrected before LST retrieval.

B. Possible Reasons for the Poor Performance of ERA5

Three stations were selected as a case study to analyze the possible reasons for poor performance of ERA5 in the Americas and Africa. The evaluation result for three stations is shown in Table V. The air temperature and relative humidity profiles at Dakar station (ID: 61641) on 15 April 2013, Lake Charles station (ID: 72240) on 15 July 2013, and Lima–Callao station (ID: 84628) on 15 July 2013 were extracted and are plotted in Fig. 4.

As shown in Fig. 4, the vertical distribution of air temperature profiles extracted from MERRA2, FNL, and ERA5 was

similar to that of radiosonde profiles. But there was a temperature difference between ERA5 and radiosonde profiles at low altitude (<800 m), which was about 5–10 K at Dakar and Lake Charles station and 1–5 K at Lima–Callao station. The relative humidity profiles extracted from different atmospheric profiles are quite different in shape. When the altitude was less than 10 km, the shape of MERRA2 (FNL) was similar to that of radiosonde profile, whereas ERA5 had a different shape whether the altitude was high or low than 10 km. The vertical distribution of air temperature and relative humidity profiles may explain the poor performance of ERA5. Moreover, the MERRA2 product has no data for low altitude (<1000 m) at the Lima–Callao station, which can explain the overestimation of atmospheric transmittance and the underestimation of atmospheric upward(downward) radiance.

V. CONCLUSION

In this letter, the accuracy and uncertainty of the ERA5 reanalysis product were evaluated using ground radiosounding profiles collected from 163 radiosonde observations. In addition, the performance of the ERA5 reanalysis product was compared with that of the MERRA2 and FNL reanalysis products. Both the overall evaluation results and the evaluation results under various groups of water vapor contents indicated that the uncertainty of atmospheric upward radiance, downward radiance, and transmittance simulated from the ERA5 reanalysis product was higher than that simulated from MERRA2 and FNL reanalysis products.

But the evaluation results in six continents indicated that the ERA5 reanalysis product performed differently over regions, with lower absolute biases and RMSEs over most regions, and higher biases and RMSEs over Americas than that of the MERRA2 and FNL reanalysis products. More exploration is needed to analyze this phenomenon in future work.

This is the first time that the performance of the ERA5 reanalysis product in the atmospheric correction of TIR data is evaluated using ground radiosounding profiles. This letter will facilitate the utility of the ERA5 reanalysis product in the atmospheric correction of a variety of TIR data.

REFERENCES

- [1] Z. Wan and J. Dozier, "A generalized split-window algorithm for retrieving land-surface temperature from space," *IEEE Trans. Geosci. Remote Sens.*, vol. 34, no. 4, pp. 892–905, Jul. 1996.
- [2] S. Xu and J. Cheng, "A new land surface temperature fusion strategy based on cumulative distribution function matching and multiresolution Kalman filtering," *Remote Sens. Environ.*, vol. 254, Mar. 2021, Art. no. 112256, doi: [10.1016/j.rse.2020.112256](https://doi.org/10.1016/j.rse.2020.112256).
- [3] M. C. Anderson, J. M. Norman, W. P. Kustas, R. Houborg, P. J. Starks, and N. Agam, "A thermal-based remote sensing technique for routine mapping of land-surface carbon, water and energy fluxes from field to regional scales," *Remote Sens. Environ.*, vol. 112, no. 12, pp. 4227–4241, Dec. 2008, doi: [10.1016/j.rse.2008.07.009](https://doi.org/10.1016/j.rse.2008.07.009).
- [4] S.-B. Duan, Z.-L. Li, B.-H. Tang, H. Wu, and R. Tang, "Generation of a time-consistent land surface temperature product from MODIS data," *Remote Sens. Environ.*, vol. 140, pp. 339–349, Jan. 2014, doi: [10.1016/j.rse.2013.09.003](https://doi.org/10.1016/j.rse.2013.09.003).
- [5] J. A. Sobrino, F. D. Frate, M. Drusch, J. C. Jiménez-Muñoz, P. Manunta, and A. Regan, "Review of thermal infrared applications and requirements for future high-resolution sensors," *IEEE Trans. Geosci. Remote Sens.*, vol. 54, no. 5, pp. 2963–2972, May 2016, doi: [10.1109/TGRS.2015.2509179](https://doi.org/10.1109/TGRS.2015.2509179).
- [6] J. Cheng and W. Kustas, "Using very high resolution thermal infrared imagery for more accurate determination of the impact of land cover differences on evapotranspiration in an irrigated agricultural area," *Remote Sens.*, vol. 11, no. 6, p. 613, Mar. 2019, doi: [10.3390/rs11060613](https://doi.org/10.3390/rs11060613).
- [7] Z.-L. Li *et al.*, "Satellite-derived land surface temperature: Current status and perspectives," *Remote Sens. Environ.*, vol. 131, pp. 14–37, Apr. 2013, doi: [10.1016/j.rse.2012.12.008](https://doi.org/10.1016/j.rse.2012.12.008).
- [8] J. A. Barsi, J. L. Barker, and J. R. Schott, "An atmospheric correction parameter calculator for a single thermal band Earth-sensing instrument," in *Proc. IEEE Int. Geosci. Remote Sens. Symp. (IGARSS)*, Toulouse, France, Jul. 2003, pp. 21–25.
- [9] B. Tardy, V. Rivalland, M. Huc, O. Hagolle, S. Marcq, and G. Boulet, "A software tool for atmospheric correction and surface temperature estimation of Landsat infrared thermal data," *Remote Sens.*, vol. 8, no. 9, p. 696, Aug. 2016, doi: [10.3390/rs8090696](https://doi.org/10.3390/rs8090696).
- [10] J. Cheng, X. Meng, S. Dong, and S. Liang, "Generating the 30-m land surface temperature product over continental China and USA from Landsat 5/7/8 data," *Sci. Remote Sens.*, vol. 4, Dec. 2021, Art. no. 100032, doi: [10.1016/j.srs.2021.100032](https://doi.org/10.1016/j.srs.2021.100032).
- [11] N. K. Malakar, G. C. Hulley, S. J. Hook, K. Laraby, M. Cook, and J. R. Schott, "An operational land surface temperature product for Landsat thermal data: Methodology and validation," *IEEE Trans. Geosci. Remote Sens.*, vol. 56, no. 10, pp. 5717–5735, Oct. 2018, doi: [10.1109/TGRS.2018.2824828](https://doi.org/10.1109/TGRS.2018.2824828).
- [12] G. C. Hulley, N. K. Malakar, T. Islam, and R. J. Freepartner, "NASA's MODIS and VIIRS land surface temperature and emissivity products: A long-term and consistent Earth system data record," *IEEE J. Sel. Topics Appl. Earth Observ. Remote Sens.*, vol. 11, no. 2, pp. 522–535, Feb. 2018, doi: [10.1109/JSTARS.2017.2779330](https://doi.org/10.1109/JSTARS.2017.2779330).
- [13] S. Zhou and J. Cheng, "An improved temperature and emissivity separation algorithm for the advanced Himawari imager," *IEEE Trans. Geosci. Remote Sens.*, vol. 58, no. 10, pp. 7105–7124, Oct. 2020, doi: [10.1109/TGRS.2020.2979846](https://doi.org/10.1109/TGRS.2020.2979846).
- [14] J. Yang *et al.*, "Evaluation of seven atmospheric profiles from reanalysis and satellite-derived products: Implication for single-channel land surface temperature retrieval," *Remote Sens.*, vol. 12, no. 5, p. 791, Mar. 2020, doi: [10.3390/rs12050791](https://doi.org/10.3390/rs12050791).
- [15] X. Meng and J. Cheng, "Evaluating eight global reanalysis products for atmospheric correction of thermal infrared sensor—Application to Landsat 8 TIRS10 data," *Remote Sens.*, vol. 10, no. 3, p. 474, Mar. 2018, doi: [10.3390/rs10030474](https://doi.org/10.3390/rs10030474).
- [16] H. Li, Q. Liu, Y. Du, J. Jiang, and H. Wang, "Evaluation of the NCEP and MODIS atmospheric products for single channel land surface temperature retrieval with ground measurements: A case study of HJ-1B IRS data," *IEEE J. Sel. Topics Appl. Earth Observ. Remote Sens.*, vol. 6, no. 3, pp. 1399–1408, Jun. 2013, doi: [10.1109/JSTARS.2013.2255118](https://doi.org/10.1109/JSTARS.2013.2255118).
- [17] L. Pérez-Planells, V. García-Santos, and V. Caselles, "Comparing different profiles to characterize the atmosphere for three MODIS TIR bands," *Atmos. Res.*, vols. 161–162, pp. 108–115, Aug. 2015, doi: [10.1016/j.atmosres.2015.04.001](https://doi.org/10.1016/j.atmosres.2015.04.001).
- [18] D. Skokovic, J. A. Sobrino, and J. C. Jimenez-Munoz, "Vicarious calibration of the Landsat 7 thermal infrared band and LST algorithm validation of the ETM+ instrument using three global atmospheric profiles," *IEEE Trans. Geosci. Remote Sens.*, vol. 55, no. 3, pp. 1804–1811, Mar. 2017, doi: [10.1109/TGRS.2016.2633810](https://doi.org/10.1109/TGRS.2016.2633810).
- [19] F. Johannsen, S. Ermida, J. Martins, I. F. Trigo, M. Nogueira, and E. Dutra, "Cold bias of ERA5 summertime daily maximum land surface temperature over Iberian Peninsula," *Remote Sens.*, vol. 11, no. 21, p. 2570, Nov. 2019, doi: [10.3390/rs11212570](https://doi.org/10.3390/rs11212570).
- [20] H. Hersbach *et al.*, *ERA5 Hourly Data on Pressure Levels from 1979 to Present, Copernicus Climate Change Service (C3S) Climate Data Store (CDS)*, 2018, Accessed: Apr. 1, 2021, [Online]. Available: <https://cds.climate.copernicus.eu/cdsapp#!/dataset/10.24381/cds.bd0915c6?tab=overview,doi:10.24381/cds.bd0915c6>.
- [21] *MERRA-2 Inst6_3D_Ana_Np: 3D, 6-Hourly, Instantaneous, Pressure-Level, Analysis, Analyzed Meteorological Fields V5.12.4*, Goddard Earth Sciences Data and Information Services Center (GES DISC), Global Modeling and Assimilation Office (GMAO), Greenbelt, MD, USA, 2015. Accessed: Dec. 31, 2016, doi: [10.5067/A7S6XP56VZWS](https://doi.org/10.5067/A7S6XP56VZWS).
- [22] *NCEP FNL Operational Model Global Tropospheric Analyses, Continuing From Jul. 1999. Research Data Archive at the National Center for Atmospheric Research, Computational and Information Systems Laboratory*, National Centers for Environmental Prediction/National Weather Service/NOAA/U.S. Department of Commerce, Washington, DC, USA, 2000. Accessed: Dec. 31, 2016, doi: [10.5065/D6M043C6](https://doi.org/10.5065/D6M043C6).
- [23] A. N. French, J. M. Norman, and M. C. Anderson, "A simple and fast atmospheric correction for spaceborne remote sensing of surface temperature," *Remote Sens. Environ.*, vol. 87, nos. 2–3, pp. 326–333, Oct. 2003, doi: [10.1016/j.rse.2003.08.001](https://doi.org/10.1016/j.rse.2003.08.001).